MOLECULAR AND CELLULAR BIOLOGY, Oct. 2007, p. 6782–6793 Vol. 27, No. 19
0270-7306/07/$08.00+0 doi:10.1128/MCB.01097-07

A Dynamic Scaffold of Pre-snoRNP Factors Facilitates Human Box C/D snoRNP Assembly▽

Kenneth Scott McKeegan,[1] Charles Maurice Debieux,[1] Séverine Boulon,[2] Edouard Bertrand,[2] and Nicholas James Watkins[1]*

ICaMB, University of Newcastle upon Tyne, Newcastle upon Tyne NE2 4HH, United Kingdom,[1] and IGMM, CNRS UMR5535, Montpellier, France[2]

Received 20 June 2007/Accepted 6 July 2007

The box C/D small nucleolar RNPs (snoRNPs) are essential for the processing and modification of rRNA. The core box C/D proteins are restructured during human U3 box C/D snoRNP biogenesis; however, the molecular basis of this is unclear. Here we show that the U8 snoRNP is also restructured, suggesting that this may occur with all box C/D snoRNPs. We have characterized four novel human biogenesis factors (BCD1, NOP17, NUFIP, and TAF9) which, along with the ATPases TIP48 and TIP49, are likely to be involved in the formation of the pre-snoRNP. We have analyzed the in vitro protein-protein interactions between the assembly factors and core box C/D proteins. Surprisingly, this revealed few interactions between the individual core box C/D proteins. However, the novel biogenesis factors and TIP48 and TIP49 interacted with one or more of the core box C/D proteins, implying that they mediate the assembly of the pre-snoRNP. Consistent with this, we show that NUFIP bridges interactions between the core box C/D proteins in a partially reconstituted pre-snoRNP. Restructuring of the core complex probably reflects the conversion of the pre-snoRNP, where core protein-protein interactions are maintained by the bridging biogenesis factors, to the mature snoRNP.

Three of the four eukaryotic rRNAs are cotranscribed as a large precursor RNA (pre-rRNA) in the nucleolus (2, 37, 46). The pre-rRNA undergoes a complex series of processing and modification steps (17) to generate the mature rRNAs. Small nucleolar RNAs (snoRNAs) are an evolutionarily conserved group of noncoding RNAs found in both eukaryotes and *Archaea* that are involved in the modification and processing of rRNAs (2, 9, 46). Based on conserved sequence elements, two classes of snoRNA have been defined; the H/ACA and box C/D snoRNAs. The majority of box C/D snoRNAs direct the 2′-O methylation of RNA by base pairing with target sequences (2, 30, 46). A subset of box C/D snoRNAs, including U3, U8, and U14, contain rRNA complementary regions that are proposed to act as chaperones in rRNA processing (reviewed in reference 46).

Box C/D snoRNAs are present in the cell as small nucleolar ribonucleoprotein particles (snoRNPs) and are associated with a common set of four core proteins: 15.5K, fibrillarin (methyltransferase), NOP56, and NOP58 (reviewed in reference 46). Association with the core box C/D proteins is essential for the accumulation of the snoRNA, as well as snoRNA processing and nucleolar localization (29). The hierarchical assembly of the eukaryotic box C/D snoRNPs in nuclear extract first involves 15.5K binding to the highly conserved k-turn element present in the box C/D motif (48, 50). Binding of 15.5K and the conserved stem II of the box C/D motif are required for the recruitment of NOP56, NOP58, and fibrillarin (48). A similar assembly pathway has been observed for the Archaeal complexes, with the 15.5K homologue L7ae binding first followed by NOP5 and fibrillarin (40). The proteins are predicted to be distributed symmetrically with one copy of L7ae, NOP5, and fibrillarin present on both the C/D and C′/D′ motifs, with the two complexes linked via a protein-protein interaction between the coiled-coil domain of the NOP5 proteins (1, 42, 47). In contrast, the proteins are predicted to be arranged asymmetrically on the eukaryotic box C/D snoRNAs, with 15.5K, NOP58, and fibrillarin contacting the C/D motif and NOP56 and fibrillarin contacting the C′/D′ motif (7).

In vertebrates most box C/D snoRNAs are encoded within the introns of protein-coding genes and are processed from the spliced intron lariat (29, 51). Intronic snoRNP assembly occurs on the pre-mRNA and is coordinated with pre-mRNA splicing (22, 23), with the binding of the helicase-like protein IBP160 to the spliceosomal C1 complex essential for the position-dependent assembly of the box C/D snoRNP (21). A subset of snoRNAs, which includes U3, U8, and U13, are independently transcribed by RNA polymerase II. The primary transcripts of these genes possess an m^7G cap structure and a short 3′ extension. During biogenesis, the cap is hypermethylated to an $m^{2,2,7}G$ cap (m_3G cap) and the short 3′ is extension removed (13, 35, 51). In vivo, biogenesis of the U3 box C/D snoRNP is mediated by a large dynamic multiprotein pre-snoRNP complex that contains proteins linked to assembly (the AAA+-like proteins TIP48 and TIP49), snoRNA processing (TGS1, La, LSm proteins, and exosome), and nucleocytoplasmic transport (PHAX, CRM1, CBC, Ran, and Nopp140) (4, 49). During U3 snoRNP biogenesis the complex undergoes a restructuring event, leading to the stabilization of the association of the core box C/D proteins, prior to or during nucleolar localization (49). The presence of TIP48 and TIP49, two putative assembly factors, in the pre-snoRNP implies that many of these events may be regulated by the hydrolysis of ATP. These two AAA+

* Corresponding author. Mailing address: Institute for Cell and Molecular Biosciences, University of Newcastle upon Tyne, Newcastle upon Tyne NE2 4HH, United Kingdom. Phone: 44 191 222 6991. Fax: 44 191 222 7424. E-mail: n.j.watkins@ncl.ac.uk.

▽ Published ahead of print on 16 July 2007.

proteins have been shown to hydrolyze ATP and are essential for box C/D snoRNA accumulation in both human and *Saccharomyces cerevisiae* (28, 49). The ability of the yeast TIP48 to bind and hydrolyze ATP is essential for the accumulation of box C/D snoRNAs (28). However, the roles of these two putative assembly factors in the organization and function of the pre-snoRNP complex are unclear.

Proteins with the ability to bind and hydrolyze nucleotides (NTPases) are required for the assembly and function of a number of RNP complexes including spliceosomal snRNP assembly, pre-mRNA splicing, and ribosome biogenesis (5, 8, 52). NTPases have been proposed to use the chemical energy derived from nucleotide hydrolysis to remodel the interactions within RNP complexes. However, the mechanistic details behind the involvement of NTP hydrolysis in RNP assembly are largely unknown. NOP56 and NOP58 undergo a remodeling and/or restructuring event within the U3 snoRNP, stabilizing their association with the complex, prior to nucleolar localization (49). TIP48 and TIP49 are the only ATPases known to be associated with the pre-snoRNPs and, as such, may be the driving force behind the change in snoRNP structure. The molecular basis of this restructuring event is unclear. Furthermore, the structural organization of the pre-snoRNP and the function of the biogenesis factors are unknown. We have analyzed the key protein-protein interactions that occur within the pre-snoRNP complex to provide insights into the functions of TIP48 and TIP49 and to further elucidate the molecular basis of box C/D snoRNP assembly and restructuring.

MATERIALS AND METHODS

DNA oligonucleotides. The DNA oligonucleotide primers were as follows: 1, GAATTCATGGCAACCGTGGCAGCCAC; 2, CTCGAGTCAGGAGGTGTC CATTGTTT; 3, GAATTCATGAAGATTGAGGAGGTGAA; 4, CTCGAGTT ACTTCATGTACTTGTCCT; 5, GAATTCATGGCGAACCCGAAGCTGCT; 6, CTCGAGTGATCAAGAAGGCACCGGCA; 7, GCGGATCCATGGAGTT TGCTGCTGAAAATGAA; 8, CGCTCGAGTCAATTTTCATTGCCAACGTT CTTGTT; 9, CGCTCGAGTCATATGTACTCAGCTTGACTTTGAGG; 10, ATGGTGCTGTTGCACGTGCTGTTTGAGCAC; 11, ATGGTGCTGTTGCA CGTGCTGTTTGAGCAC; 12, ATGTTGGTGCTGTTTGAAACGTCTGTG GGT; 13, TAGGAGCAAGAGAGAGAAAAAAAAGAAAAAGAAGAAA; 14, AGTAATCTCAGCAGCCGCTTCC; 15, AGAGCAGGTTGGAAGTGTG GAGTC; 16, GCGGATCCATGAAGCCAGGATTCAGTCCC; and 17, GCG AGCTCTCAGTTCTTCACCTTGGGGGGTGGCC.

Constructs. The pET15b mouse TIP48 and TIP49 plasmids were kindly provided by Stuart Maxwell (38). Mouse TIP48 and TIP49 were PCR amplified by using primers 1 and 2 and 3 and 4 and cloned into the EcoRI and XhoI sites of pGEX-6P-1. Human NOP17 (accession number NM_017916) was PCR amplified from a full-length cDNA clone (Geneservice) by using primers 5 and 6, cloned into pGEM-T Easy and then subcloned into the EcoRI and XhoI sites of pGEX-6P-1. A cDNA clone of human BCD1 (accession number BC026236) was kindly supplied by Edouard Bertrand. Full-length BCD1 and the coding region corresponding to amino acids 1 to 360 [BCD1(1-360)] were PCR amplified with primer pairs 7/8 and 7/9, respectively. The coding region of BCD1(1-360) was then subcloned into the BamHI and XhoI sites of pGEX-6P-2. Clones for human NOP56 (15) and NOP58 (34) were kindly supplied by Ed Hurt and Susan Baserga, respectively. NOP56 and NOP58 cDNAs were PCR amplified by using the primer pairs 10/11 and 12/13, respectively, and cloned into pCRT7-TOPO. The coding regions of NOP56 (amino acids 1 to 458) and NOP58 (amino acids 1 to 435) were PCR amplified by using primer pairs 10/14 and 12/15, respectively, and cloned into pBAD/Thio-TOPO. pGEX4T2-15.5K and pGADT7-15.5K were kindly supplied by Reinhard Luhrmann (33, 39). Glutathione *S*-transferase (GST)-tagged TAF9 and pET-TAF9 were supplied by Robert Tjian (31). pGEX2T-NUFIP and pcDNA-NUFIP were kindly supplied by Pavel Cabart (6). pCINeoVSV-fibrillarin was kindly supplied by Sander Granneman and Ger Pruijn. The fibrillarin coding sequence was amplified by using primes 16 and 17 and cloned into the BamHI/XhoI sites of pGEX-6P-1.

Protein purification. All GST- and His-tagged proteins were overexpressed in *Escherichia coli* BL21. The thioredoxin-tagged proteins were expressed in TOP10 cells. GST-tagged fusion proteins were purified by glutathione-Sepharose chromatography. His-tagged and thioredoxin-tagged fusion proteins were purified by immobilized metal affinity chromatography. GST-tagged TIP48 and TIP49 were purified in buffer A (20 mM Tris-HCl [pH 8.0], 10% glycerol, 300 mM KCl, 0.1% Tween 20, 1 mM Tris-hydroxy-phosphine). All other proteins were purified in buffer B (20 mM Tris-HCl [pH 8.0], 10% glycerol, 200 mM NaCl, 0.1% Triton X-100, 1 mM Tris-hydroxy-phosphine).

Protein-protein interaction studies. [^{35}S]methionine-labeled proteins were all produced by coupled in vitro transcription and translation in rabbit reticulocyte lysate, as described by the manufacturer (Promega). Equal amounts of GST-bait proteins were immobilized on glutathione-Sepharose beads, and the target proteins were then added. All binding reactions were carried out for 2 h at 4°C in buffer A (GST-TIP48 and GST-TIP49) or buffer B (all other proteins). The beads were washed in the appropriate buffer, and the retained proteins separated on a 12% polyacrylamide sodium dodecyl sulfate (SDS) gel and visualized either by autoradiography or Coomassie staining. All interaction experiments were repeated a minimum of three times.

Antibodies, immunoprecipitation, and immunoblotting. Rabbits were immunized with either GST-NOP17 or a truncated form of BCD1, GST-BCD(1-360) that contains amino acids 1 to 360, respectively. Recombinant proteins coupled to *N*-hydroxysuccinimide-activated Sepharose were used to purify the antibodies. Anti-NOP56 antibodies were as previously described (49). TAF9 and fibrillarin antibodies were purchased from Santa Cruz Biotechnology. Antibodies recognizing NUFIP were supplied by Barbara Bardoni (3). HeLa nuclear extracts were prepared according to the method of Dignam et al. (10). HeLa nucleolar extracts were prepared as previously described (49), with the extracts prepared by sonication in a final buffer of 20 mM HEPES-NaOH (pH 7.9), 150 mM NaCl, 0.2 mM EDTA, 0.5 mM dithiothreitol, and 10% glycerol. Immunoprecipitations and immunoblotting were carried out as previously described (49). Immunopurification was performed with purified anti-NOP58 antibodies immobilized on protein A-Sepharose (50). HeLa nuclear extract was incubated with the immobilized antibodies, and the bound material was eluted by using an excess of the peptide epitope. The eluate was then analyzed by SDS-polyacrylamide gel electrophoresis (PAGE) and Western blotting.

siRNA transfection and cell culture. All small interfering RNA (siRNA) duplexes were designed as 21-mers with 3′dTdT overhangs (11). For the BCD1 knockdown, siRNA duplexes targeting the sequences GGAGACGGATAGUA GTTTA and GGAGAAGTTTGTTGGTCAA in the cDNA were used. For NOP17, siRNA duplexes targeting the sequences CGATGGTGTTCGGTC TTGA and GTAGGTATCCGGAGTCGAT in the cDNA were used. NOP58 and fibrillarin depletion was performed as previously described (49). The GL2 siRNA (which targets the firefly luciferase gene) was used as a control (11). The depletion of hPRP31 was performed as described previously (44). At 60 h after transfection either the cells were harvested and the protein and RNA content analyzed by Western and Northern blotting, respectively, or the cells were fixed and analyzed by in situ hybridization using fluorescent U3, U4, and U2 antisense probes as previously described (18, 44). The same exposure time was used for each fluorescent probe to allow direct comparison of the subcellular distribution of the RNA after the depletion of specific factors.

In vitro assembly of a partial pre-snoRNP. For assembly of the partial pre-snoRNP complex, the polyhistidine-tagged thioredoxin fusion proteins of NOP56(1-458) or NOP58(1-435) were immobilized on MagZ beads (Invitrogen). GST-NUFIP and wild-type 15.5K were added sequentially in buffer B, prior to addition of in vitro-transcribed ^{32}P-labeled U14 or U14 MutC (49). All incubations were carried out at 4°C for 2 h. Bound RNA was separated on an 8% polyacrylamide–7 M urea gel and analyzed by autoradiography.

RESULTS

Restructuring of the U8 box C/D snoRNP during biogenesis. A significant difference in the salt stability of the association of NOP56 and NOP58 with the U3 pre-snoRNP and mature snoRNP complexes suggested that the core box C/D complex undergoes a remodeling or restructuring event during biogenesis (49). In order to determine whether this observation is specific to the U3 snoRNP, we compared the association of the core snoRNP proteins NOP56 and NOP58 with the U8 box

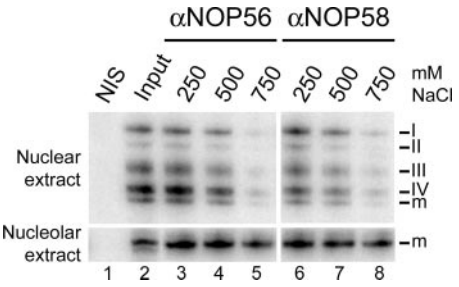

FIG. 1. Nuclear and nucleolar core U8 box C/D snoRNPs exhibit different salt stabilities. U8 snoRNPs present in either nuclear (upper panel) or nucleolar (lower panel) extract were immunoprecipitated with nonimmune serum (NIS) or antibodies to either NOP56 or NOP58. Bound particles were incubated with buffer containing 250, 500, or 750 mM NaCl, as indicated. The associated U8 snoRNAs were isolated, separated on an 8% polyacrylamide–7 M urea gel, and analyzed by Northern blotting. The U8 pre-snoRNAs (I to IV) and mature snoRNA (m) present in nuclear extracts are indicated on the right of the panel. Input represents 10% of the starting material. The antibody used is indicated at the top of the panel.

C/D snoRNA in pre-snoRNP and mature snoRNP complexes at different salt concentrations.

Nuclear extract, prepared as described previously (10), contains only minimal levels of mature snoRNP complexes (49). The nucleoli, containing the bulk of the mature snoRNPs, are removed from nuclear extracts during the final centrifugation steps of this preparation process. Therefore, by comparing extracts derived from nucleoli and nuclei, we are able to independently analyze the mature and pre-snoRNP complexes, respectively. U8 snoRNPs were immunoprecipitated from either nucleolar or nuclear extracts using anti-NOP56 or anti-NOP58 antibodies. The bound material was then washed with increasing concentrations of NaCl (Fig. 1). RNAs remaining bound to the beads were eluted and analyzed by Northern hybridization.

Nuclear extract contains four U8 precursor RNAs (Fig. 1, I to IV) and the mature-length transcript (Fig. 1, m). The precursor RNAs each contain an m^7G cap and have 3′ extensions of between 4 and 25 nucleotides (49a). All forms of the U8 snoRNA in the nuclear extract complexes were stably associated with both NOP56 and NOP58 at 250 mM NaCl (Fig. 1, upper panel). However, at higher salt concentrations the U8 snoRNA and pre-snoRNAs dissociated from the bound NOP56 and NOP58 (lanes 5 and 8). Quantitation of the data revealed that, for both proteins, there was a >10-fold decrease in U8 snoRNA association upon increasing the NaCl concentration from 250 to 750 mM (Fig. 1, upper panel). The dissociation observed was equivalent for both the mature length and pre-U8 snoRNAs present in nuclear extracts. Therefore, the association of the core proteins NOP56 and NOP58 with the U8 snoRNA in nuclear extract is salt sensitive. In contrast, less than a twofold difference was observed for the association of NOP56 and NOP58 to mature nucleolar U8 snoRNP incubated at 250 and 750 mM NaCl (Fig. 1, lower panel, lanes 2 to 8). This demonstrates a significant difference in the stability of the U8 core snoRNP between complexes found in the nucleoplasm and the nucleolus, suggesting that the core box C/D proteins in the U8 snoRNP are also restructured during biogenesis.

A limited number of interactions between individual core box C/D proteins. Defining the protein-protein interactions that occur during snoRNP biogenesis is essential to understanding the molecular basis of the restructuring of the core box C/D complex. We therefore analyzed the interactions between the individual core box C/D snoRNP proteins. Purified GST-15.5K, GST-fibrillarin, or GST alone (Fig. 2A) were immobilized on glutathione-Sepharose resin and then incubated with in vitro-translated ^{35}S-labeled 15.5K, fibrillarin, NOP56, or NOP58. The beads were washed, and the bound material was analyzed by SDS-PAGE followed by autoradiography. This revealed that NOP56, but not NOP58, fibrillarin, or 15.5K, was retained by the immobilized GST-fibrillarin (Fig. 2B, lane 4). GST-15.5K did not detectably bind any of the ^{35}S-labeled box C/D core proteins (Fig. 2B, lane 3). GST, which was used as a negative control, did not retain any of the ^{35}S-labeled core proteins (Fig. 2B, lane 2). This shows that fibrillarin specifically interacts with NOP56, supporting earlier evidence of an interaction between these two proteins in *Saccharomyces cerevisiae* (15, 32). Importantly, 15.5K and the core box C/D proteins (either in vitro translated or purified recombinant proteins) also did not interact in the presence of a box C/D snoRNA in either GST-pull-down or gel-shift experiments (see Fig. 6; also data not shown), suggesting that additional factors are likely required to form a box C/D snoRNP.

The ATPases TIP48 and TIP49 interact with fibrillarin and 15.5K. TIP48 and TIP49 are two putative assembly factors associated with the box C/D pre-snoRNP complexes that could potentially bridge interactions between the core box C/D proteins. We therefore analyzed the interactions between TIP48 and TIP49 and the core box C/D proteins. GST-TIP48, GST-TIP49, or GST alone (Fig. 2A) were immobilized on glutathione-Sepharose beads and then incubated with in vitro-translated ^{35}S-labeled 15.5K, fibrillarin, NOP56, and NOP58. Bound proteins were analyzed by SDS-PAGE and autoradiography. GST-TIP48 and GST-TIP49 both retained fibrillarin (Fig. 2C, lanes 3 and 4) but failed to interact with 15.5K, NOP56, and NOP58. Since nucleotide binding often induces conformational changes in AAA+ proteins, thereby altering their substrate specificity (12), reactions were also performed in the presence of 1 mM concentrations of either ATP or ADP. We observed nucleotide-dependent binding of 15.5K with both TIP48 and TIP48 (data not shown) but not with NOP56 and NOP58. The association of fibrillarin with the two ATPases was not significantly altered by the addition of nucleotide. The reticulocyte lysate used to generate the ^{35}S-labeled proteins contains nucleotides that may influence the interaction between the proteins. We therefore examined the interaction between GST-15.5K and recombinant, purified TIP48 and TIP49.

GST-15.5K or GST alone (Fig. 2D) were immobilized on glutathione-Sepharose beads and then incubated with recombinant purified TIP48 or TIP49 either alone or in the presence of 1 mM ATP or ADP. The bound proteins were eluted, separated by SDS-PAGE, and then revealed by Coomassie blue staining. In the absence of nucleotide the binding of TIP48 and TIP49 to GST-15.5K was barely detectable and not significantly higher that that seen for GST alone. In contrast, the addition of ATP resulted in a clear interaction between 15.5K and both TIP48 and TIP49. Interestingly, these interac-

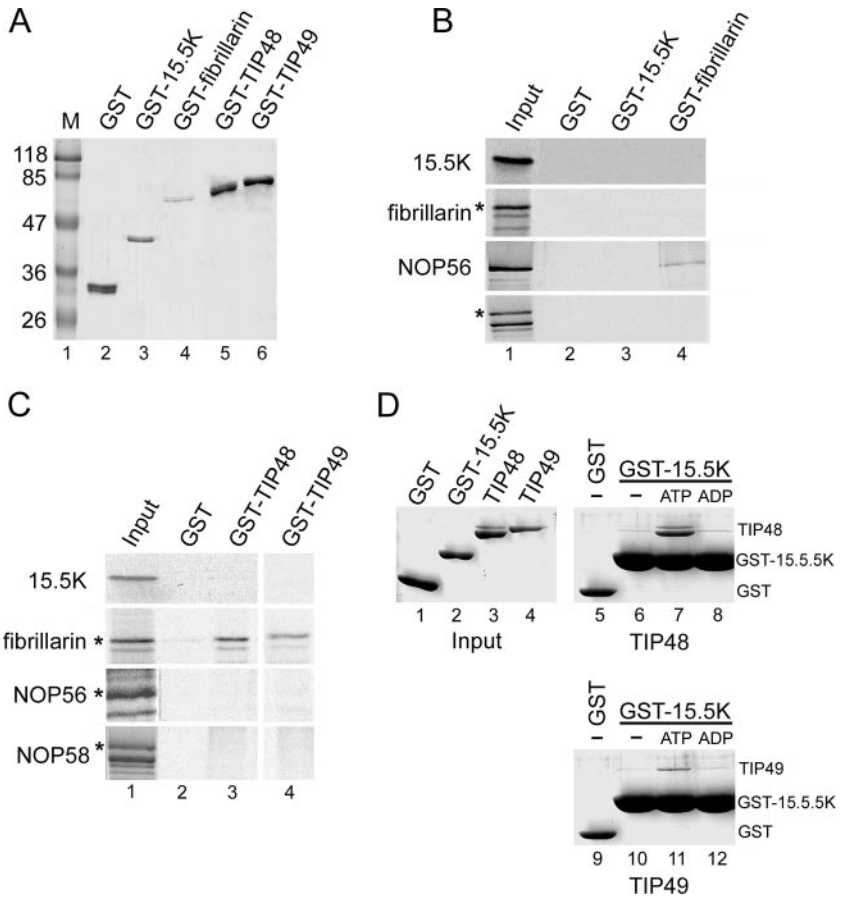

FIG. 2. Protein-protein interactions between the known pre-snoRNP factors. (A) Recombinant GST, GST-15.5K, GST-fibrillarin, GST-TIP48, and GST-TIP49 were separated on an SDS–12% polyacrylamide gel and visualized by Coomassie staining. The identity of the protein loaded is indicated at the top of the gel. M, molecular weight marker. The sizes of the molecular mass marker bands are indicated at the left of the panel in kilodaltons. (B and C). Equal amounts of GST, GST-15.5K, and GST-fibrillarin (B) or GST, GST-TIP48, and GST-TIP49 (C) were bound to glutathione-Sepharose and incubated with in vitro-translated [^{35}S]methionine-labeled 15.5K, fibrillarin, NOP56, and NOP58. GST-TIP48 and GST-TIP49 immobilized on glutathione-Sepharose were incubated with the ^{35}S-labeled proteins. Bound proteins were purified, resolved on an SDS-PAGE gel, and visualized by autoradiography. The identity of the GST-tagged protein used is indicated above each lane. The identity of the radiolabeled protein is indicated on the left of the panel. The full-length protein is indicated by an asterisk. Input, 10% of the ^{35}S-labeled input material. Note that a single exposure of one gel is used for each individual protein translate. (D) Recombinant, purified GST or GST-15.5K was bound to glutathione-Sepharose and then incubated with either recombinant TIP48 or TIP49 either alone or in the presence of ATP or ADP. Bound proteins were then separated by SDS-PAGE and visualized by Coomassie blue staining. "Input" indicates the proteins added to the assay. The GST-tagged protein and nucleotide used are indicated at the top of each lane. The migration of the individual proteins is indicated on the right of each panel.

tions were not stimulated by the addition of ADP. Furthermore, significantly more TIP48 than TIP49 was bound by GST-15.5K. These data indicate that TIP48 and TIP49 make dynamic, nucleotide-dependent interactions with 15.5K during box C/D snoRNP biogenesis.

Four novel biogenesis factors are associated with native box C/D pre-snoRNPs. Previously published data linked TIP48 and TIP49 recruitment to the snoRNP with that of NOP56 and NOP58 (45, 48). Furthermore, while previous work has suggested that protein-protein interactions are essential for box C/D snoRNP assembly (45), our interaction data suggest limited interactions between the box C/D core proteins and TIP48 and/or TIP49. One possible explanation for these data is that the interactions between TIP48/TIP49 and NOP56/NOP58 are indirect and mediated by other, as-yet-unidentified, pre-snoRNP proteins. Therefore, we next screened the available databases to identify factors that could bridge the interactions between the core box C/D proteins and/or TIP48 and TIP49. Three candidate proteins in *S. cerevisiae* were identified: NOP17, TAF9, and BCD1. Yeast NOP17 interacts with TIP48, TIP49, and NOP58 and is important for ribosome biogenesis (16, 54, 55). TAF9 has a histone H3-like fold and interacts with NOP56 in a yeast two-hybrid screen (25), and BCD1 is a zinc-finger protein required for yeast box C/D snoRNA accumulation (20, 41). In addition, NUFIP, a zinc finger containing transcription factor shown to associate with the fragile X mental retardation protein (FMR1) (3, 6), was recently shown to be involved in box C/D snoRNP biogenesis through an interaction with 15.5K (S. Boulon and E. Bertrand, unpublished data).

We next analyzed whether these putative snoRNP biogenesis factors were present in native pre-snoRNP complexes. As discussed above, nuclear extracts prepared by the method of

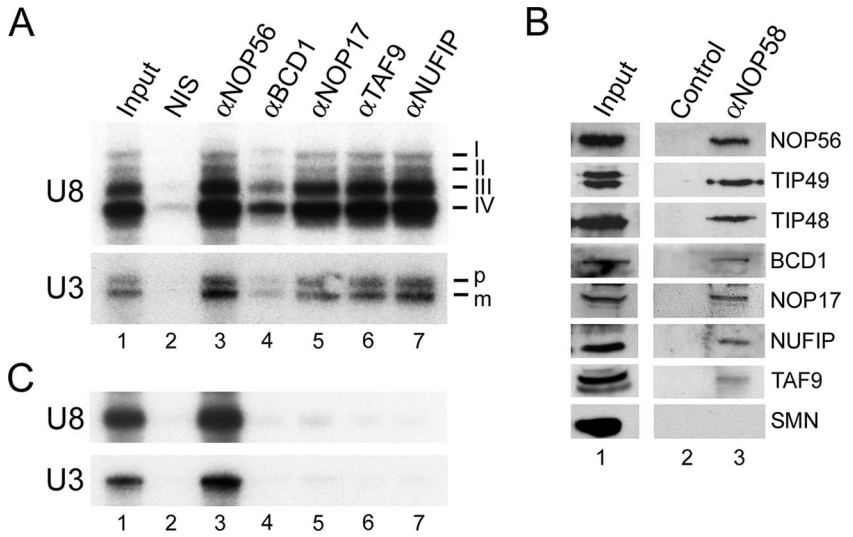

FIG. 3. Four novel factors associated with U3 and U8 pre-snoRNP complexes. Nuclear (A) or nucleolar (C) extract was immunoprecipitated with either protein-specific antibodies or control nonimmune serum (NIS). Bound RNAs were isolated and separated on an 8% polyacrylamide–7 M urea gel, and the U3 and U8 snoRNAs were revealed by Northern blotting. The antibody used is indicated at the top of each lane. The RNA analyzed is indicated to the left of each panel. The precursor U3 (p) and U8 (I to IV) and mature length transcripts (m) are indicated on the right of each panel. Input, 10% of the material used for immunoprecipitation. (B) NOP58-containing complexes were immunopurified from nuclear extract using anti-NOP58 or control IgG antibodies, and the bound material was released using an excess of the NOP58 epitope peptide. The bound material was then separated by SDS-PAGE and analyzed by Western blotting. The antibody used is indicated above each lane. Input, 10% of the starting nuclear extract. The antibodies used for Western blotting are indicated on the right.

Dignam et al. (10) contain only minimal levels of mature snoRNPs, allowing the characterization of factors associated during box C/D snoRNP biogenesis (49). HeLa nuclear extract was analyzed by immunoprecipitation with antibodies raised against either NUFIP (3) or the human homologues of BCD1, NOP17, and TAF9. Coprecipitated RNAs were purified, separated by PAGE, and analyzed by Northern blot hybridization using probes specific for U3 and U8 snoRNAs. A precursor (U3-p), containing an m^7G cap and short 3′ extension, and a mature form (U3-m) of the U3 snoRNA are present in HeLa nuclear extracts (49). In addition, four precursor forms (I to IV) and a mature form (m) of the U8 snoRNA are also found in nuclear extracts (note that levels of precursor and mature length snoRNAs vary from extract to extract [49a]). Anti-NOP56, NOP17, TAF9, and NUFIP antibodies all efficiently coprecipitated both U3-p and U3-m and all four U8 snoRNA precursors present in the nuclear extract (Fig. 3A). Our analysis of the association of NUFIP with native pre-snoRNPs confirms immunoprecipitation data using transfected cells expressing tagged NUFIP (Boulon and Bertrand, unpublished). Anti-BCD1 antibodies efficiently coprecipitated both forms of the U3 snoRNA and all four U8 pre-snoRNAs at levels significantly higher than with the control serum (NIS), although to a lesser extent than seen with the other antibodies. We therefore conclude that BCD1, NOP17, TAF9, and NUFIP are all associated with both U3 and U8 pre-snoRNPs. Both U3 and U8 pre-snoRNAs are present in large, multiprotein complexes, and the association of the four novel proteins with all forms of U8 and U3 pre-snoRNPs indicates that these proteins, like NOP56 and NOP58, are associated through much, if not all, of the biogenesis pathway.

In order to confirm that the novel biogenesis factors are present in complexes with NOP56 and NOP58, nuclear extract was incubated with immobilized anti-NOP58 antibodies. Bound NOP58 complexes were eluted using the epitope peptide and analyzed by SDS-PAGE and Western blotting. As a control, the experiment was also performed with a control purified immunoglobulin G (IgG). The NOP58 antibodies copurified NOP56, TIP48, TIP49, BCD1, NOP17, NUFIP, and TAF9 (Fig. 3B). In contrast, the survival of motor neuron protein (SMN) was not present in the anti-NOP58 column eluate. No detectable protein was eluted from the control IgG. This therefore shows that NOP58 is associated with the biogenesis factors BCD1, NOP17, NUFIP, TAF9, TIP48, and TIP49.

We next analyzed whether these proteins were also associated with mature snoRNPs. HeLa nucleolar extracts were immunoprecipitated with NOP56, BCD1, NOP17, TAF9, and NUFIP antibodies and the coprecipitating RNAs analyzed as described above. The nucleolar U3 and U8 snoRNAs were isolated by anti-NOP56 antibodies. In contrast, antibodies that recognized BCD1, NOP17, TAF9, and NUFIP only isolated background levels of mature U3 and U8 snoRNA equivalent to that seen with the control serum, suggesting that they are not associated with the mature nucleolar complexes (NIS; Fig. 3C). The association of the four novel proteins with the pre-snoRNP complexes, but not the mature snoRNPs, suggests that they are involved in box C/D snoRNP biogenesis.

BCD1 and NOP17 are essential for maintaining box C/D snoRNA levels. We next used RNA interference (RNAi) to determine the importance of the novel factors in box C/D snoRNP biogenesis. HeLa cells were transiently transfected with siRNA duplexes targeting BCD1, NOP17, and NOP58. After 60 h of incubation, the cells were harvested, and the RNA and protein content was analyzed. Western blot analysis confirmed that the transfected siRNA duplexes significantly reduced the levels of the target protein (Fig. 4A) (49). In

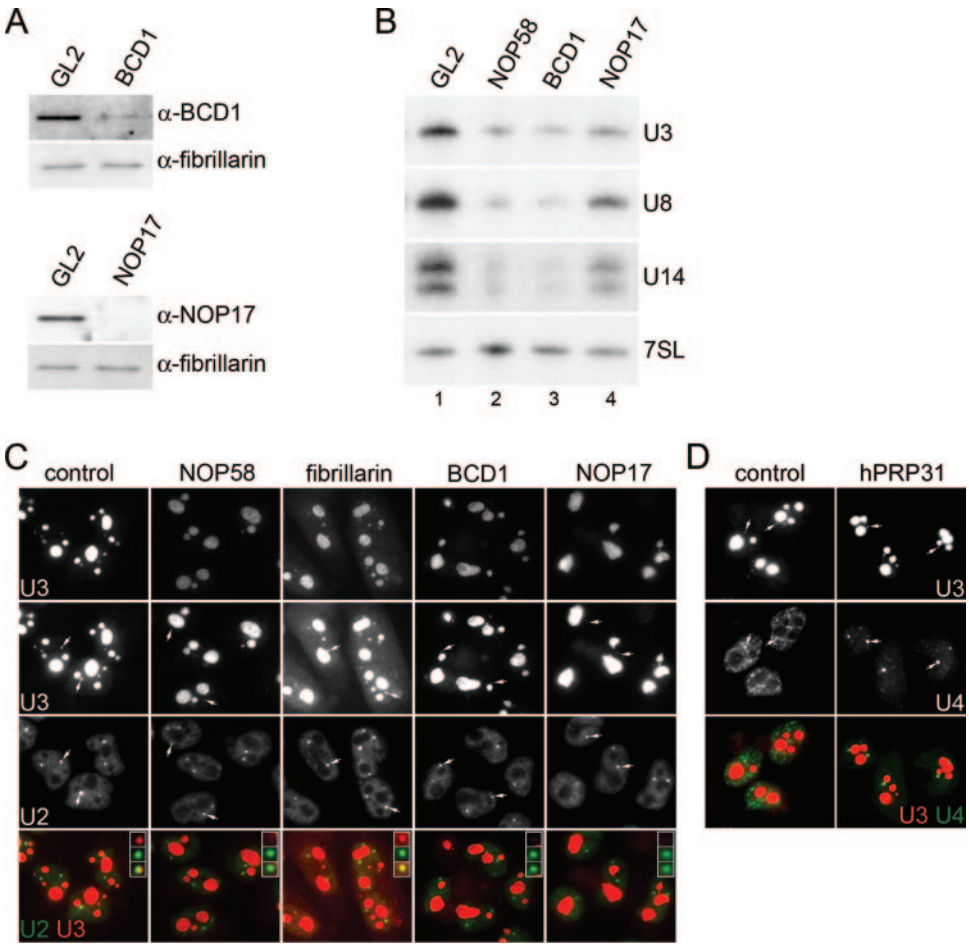

FIG. 4. BCD1 and NOP17 are essential for the maintenance of box C/D snoRNA levels. HeLa cells were treated with siRNA duplexes targeting either NOP58, fibrillarin, BCD1, NOP17, hPRP31, or the control siRNA targeting luciferase (GL2). Cells were analyzed 60 h after transfection. (A) Material derived from equal numbers of cells was analyzed by Western blotting to confirm protein depletion. The protein targeted is indicated above each panel. The antibodies used are indicated on the right. (B) Total RNA was extracted from an equal number of HeLa cells and analyzed by Northern blotting to determine the relative levels of the U3, U8, and U14 box C/D snoRNAs and the 7SL RNA. The specific probe used is indicated to the right of each panel. The protein targeted is indicated at the top of the panel. (C) Transfected HeLa cells were hybridized with fluorescent oligonucleotides complementary to the U3 snoRNA and the U2 snRNA and images captured by fluorescence microscopy. The same exposure time was used for each fluorescent probe to allow the direct comparison of the subcellular distribution of the RNA after the depletion of specific factors. The protein targeted is indicated at the top of each column of images. The first and second row of images from the top of the figure represent short and long exposures of pictures of the U3 snoRNA, respectively. The third row shows the U2 snRNA. The fourth row shows an overlay of the U2 snRNA and the long exposure of the U3 snoRNA images, respectively, for each series of cells. White arrows indicate examples of Cajal bodies. The inset panels in the bottom row of images shows a magnified view of a single Cajal body. (D) HeLa cells were transfected with siRNAs targeting hPRP31 or the control GL2 siRNA and hybridized with fluorescent oligonucleotides complementary to the U3 snoRNA and the U4 snRNA, and images were captured by fluorescence microscopy as described above. White arrows indicate examples of Cajal bodies. The protein targeted is indicated at the top of each column of images.

contrast, fibrillarin levels were not affected, confirming the specificity of the siRNA-mediated depletion (Fig. 4A). Northern blot analysis revealed that RNAi-mediated depletion of BCD1 and NOP58 resulted in a significant reduction in U3, U8, and U14 levels relative to cells transfected with the control GL2 duplex (Fig. 4B). Depletion of NOP17 resulted in an overall reduction in box C/D snoRNA levels, with a greater effect on U3 than on U8 and U14 snoRNAs, but the overall effect was not as profound as that seen with NOP58 and BCD1 (Fig. 4B). Importantly, the levels of the unrelated 7SL RNA were not affected by the knockdown of any of the proteins tested, indicating that the effects observed are specific to the box C/D snoRNAs (Fig. 4B). We conclude that BCD1 and NOP17 are important for the biogenesis of box C/D snoRNPs. We have also used RNAi to knock down TAF9. However, due to its role in RNA polymerase II transcription, we were not able to assess the importance of TAF9 in box C/D snoRNP biogenesis (data not shown). Furthermore, RNAi-mediated depletion of NUFIP resulted in a specific reduction of U3 snoRNA levels (Boulon and Bertrand, unpublished).

We next analyzed the role of BCD1 and NOP17 in U3 snoRNP localization in vivo. HeLa cells were transfected with siRNAs and, after 60 h, the cells were fixed and analyzed by fluorescence in situ hybridization with probes specific for the U3 snoRNA and the spliceosomal U2 snRNA. As a comparison, cells were also transfected with siRNAs targeting NOP58,

fibrillarin, and the control duplex targeting luciferase (GL2). The U3 snoRNA was primarily nucleolar, with signals also seen in the Cajal bodies in untransfected cells (data not shown) and cells transfected with the control GL2 siRNAs (Fig. 4C). Depletion of either NOP58 or BCD1 resulted in a strong reduction of nucleolar U3 snoRNA levels, while the loss of fibrillarin and NOP17 had a less severe effect (Fig. 4C, upper panel). This is consistent with the Northern blot analysis of total U3 snoRNA levels in transfected cells (Fig. 4B) (49). The loss of fibrillarin resulted in an increase in nucleoplasmic U3 signals while not noticeably changing the levels of the snoRNA in the Cajal body. In contrast, depletion of NOP58, BCD1, and NOP17 resulted in the significant reduction of U3 signals in the Cajal body and no noticeable snoRNA accumulation in the nucleoplasm (Fig. 4C). With the depletion of NOP58, fibrillarin, BCD1, and NOP17, the main U3 snoRNA signal observed was in the nucleolus (Fig. 4C). This signal represents either snoRNAs that have yet to be turned over, i.e., that were present in the cell prior to transfection, or a low level of snoRNAs that have been synthesized in the presence of reduced levels of the target protein. RNAi-mediated loss of NOP58, fibrillarin, BCD1, and NOP17 did not change the nucleocytoplasmic distribution of the U2 snRNA, indicating that the effects seen are specific to the U3 snoRNA (Fig. 4C).

We next analyzed the effect of depleting the essential pre-mRNA splicing factor hPRP31 on U3 snoRNA levels and localization. In particular, we wanted to determine whether or not the results we had observed were an indirect effect seen upon the loss of an essential protein. hPRP31 is homologous to both NOP56 and NOP58 and important for tri-snRNP formation. The tri-snRNP is distributed between the speckles and Cajal bodies in normal cells, and loss of hPRP31 causes the loss of the speckle localization and enrichment of tri-snRNP factors in the Cajal bodies (44). Cells were transfected with siRNAs targeting either the control GL2 siRNAs or siRNAs targeting hPRP31. At 60 h after transfection the cells were fixed and analyzed by fluorescence in situ hybridization with probes specific for the U3 snoRNA and the spliceosomal U4 snRNA. In the control cells the U4 snRNA was evenly distributed between the Cajal bodies and the speckles (Fig. 4D). Upon loss of hPRP31, the U4 was predominantly localized to the Cajal body consistent with previously published work (44). In contrast, the loss of hPRP31 did not affect the distribution of the U3 snoRNA in the cell. The U3 snoRNA was present predominantly in the nucleolus and at low levels in the Cajal bodies in both the control and hPRP31-depleted cells (Fig. 4D). This, therefore, indicates that the changes in U3 snoRNA levels and localization seen upon the RNAi-mediated depletion of NOP58, fibrillarin, NOP17, and BCD1 are specific to the functions of these proteins.

TAF9 and NUFIP interact with BCD1. We next investigated potential protein-protein interactions between BCD1, NUFIP, NOP17, and TAF9. GST-tagged NUFIP and TAF9 (6, 31) were incubated with in vitro-translated ^{35}S-labeled BCD1, NOP17, NUFIP, and TAF9 as described above. Full-length BCD1 expressed in *E. coli* as either a histidine-tagged or GST-tagged fusion protein was not soluble. As an alternative we used a GST-tagged fragment of BCD1 [BCD1(1-360); amino acids 1 to 360] in this assay (Fig. 5A, lane 6). GST-NUFIP bound BCD1 and NUFIP but not NOP17 and TAF9 (Fig. 5B, lane 4), while GST-TAF9 retained BCD1 and very low levels of NUFIP but did not bind NOP17 and TAF9 (lane 5). The weak interaction between NUFIP and TAF9, which was not much above background levels (Fig. 5B, compare lanes 2 and 5), could only be seen when using GST-TAF9. We therefore require further information before we can conclude that TAF9 interacts with NUFIP. GST-BCD1(1-360) interacted with both full-length ^{35}S-labeled BCD1 and NUFIP, but not with TAF9 and NOP17 (Fig. 5B, lane 3). The interaction between TAF9 and BCD1 was only seen when the full-length ^{35}S translate was used. However, since the GST-BCD(1-360) protein is not full length and is lacking 111 amino acids of the C terminus, it is not unreasonable to suggest that TAF9 interacts with the missing region of the protein. Taken together, these data suggest that NUFIP interacts with BCD1 and that both NUFIP and BCD1 are capable of multimerization.

The novel pre-snoRNP factors interact with TIP48 and TIP49. We next investigated whether the novel snoRNP biogenesis factors interacted with TIP48 and/or TIP49. GST-NUFIP, GST-TIP48, and GST-TIP49 were immobilized on glutathione-Sepharose and incubated with either in vitro-translated ^{35}S-labeled TIP48, TIP49, or TAF9, and the bound proteins were analyzed as described above. TIP48 was efficiently retained by GST-TIP49 (Fig. 5C), and TIP49 was efficiently bound by GST-TIP48 (data not shown). In contrast, TIP48 and TIP49 interacted about 10-fold less efficiently with GST-TIP48 and GST-TIP49, respectively. GST-TIP48 and GST-TIP49 retained TAF9 (Fig. 5C). Both TIP48 and TIP49 were bound, albeit weakly, by GST-NUFIP at levels significantly higher than with the control GST protein (Fig. 5D).

Purified, recombinant proteins were next used to investigate the interactions between TIP48, TIP49, BCD1, and NOP17. GST-BCD1(1-360), GST-NOP17, or GST (Fig. 5A) were immobilized on glutathione resin and then incubated with TIP48 or TIP49 alone or in the presence of ATP or ADP. The bound proteins were separated by SDS-PAGE and visualized by Coomassie staining. GST-BCD1(1-360) efficiently bound TIP48 in the presence of ADP (Fig. 5E, lane 4). A weaker interaction was observed in the presence of ATP and the interaction was barely detectable in the absence of nucleotide (lanes 2 and 3). A weak interaction was observed between GST-BCD1(1-360) in the presence of ATP but not with ADP or without nucleotide (Fig. 5, lanes 6 to 8). GST-NOP17 did not bind TIP48 under any of the conditions tested (Fig. 5F, lanes 2 to 4). In contrast, GST-NOP17 interacted efficiently with TIP49 either alone or in the presence of nucleotide (Fig. 5F, lanes 6 to 8). These data therefore show that NOP17 specifically interacts with TIP49 and that the interaction between BCD1 and both TIP48 and TIP49 can be regulated by the bound nucleotide.

Interactions between the novel pre-snoRNP factors and the core box C/D proteins. We next tested whether the four novel snoRNP biogenesis factors could interact with the core box C/D proteins. GST-BCD1(1-360), NOP17, NUFIP, and TAF9 were incubated with ^{35}S-labeled in vitro-translated core box C/D proteins and the bound proteins analyzed as described above. GST-NOP17, GST-BCD1(1-360), and GST-TAF9 efficiently bound fibrillarin (Fig. 5G) but not 15.5K, NOP56, or NOP58. Strikingly, GST-NUFIP efficiently bound all four core box C/D proteins (Fig. 5G, lane 4). GST-15.5K bound full-length BCD1 (data not shown), indicating that the zinc finger

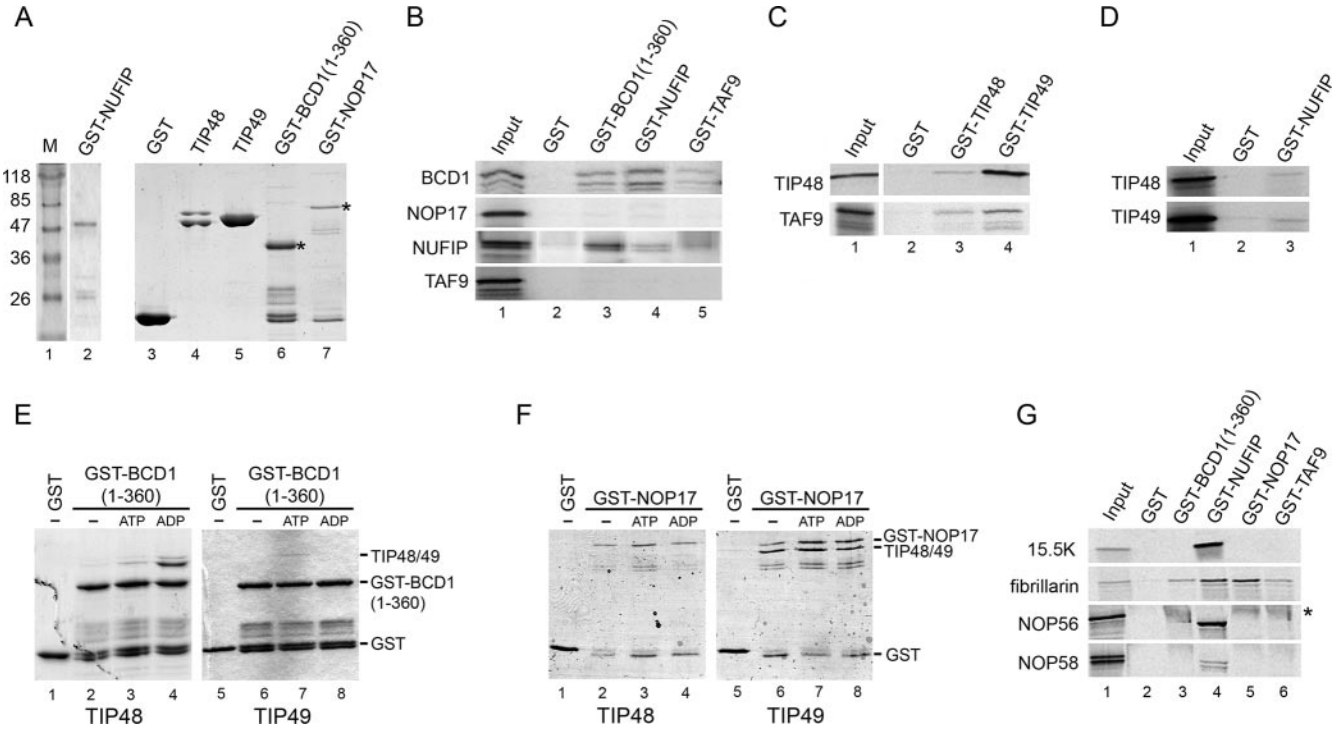

FIG. 5. Interactions between pre-snoRNP and core box C/D proteins. (A) SDS-PAGE analysis of recombinant protein inputs GST-NUFIP, GST, TIP48, TIP49, GST-BCD1(1-360), and GST-NOP17. Proteins were visualized by Coomassie blue staining. The protein loaded is indicated at the top of the gel. M, molecular weight marker. The sizes are indicated in kilodaltons to the left of the panel. Where appropriate, full-length proteins are indicated by an asterisk. (B) ^{35}S-labeled BCD1, NOP17, NUFIP, and TAF9 were incubated with immobilized GST, GST-BCD1(1-360), GST-NUFIP, or GST-TAF9. (C) ^{35}S-labeled TIP48 and TAF9 were incubated with GST, GST-TIP48, or GST-TIP49. (D) ^{35}S-labeled TIP48 and TIP49 were incubated with GST-NUFIP immobilized on glutathione-Sepharose. (E and F) Recombinant, purified GST, GST-BCD1(1-360) (E), or GST-NOP17 (F) were bound to glutathione-Sepharose and then incubated with either recombinant TIP48 or TIP49 (indicated below each panel) either alone or in the presence of ATP or ADP. Bound proteins were then separated by SDS-PAGE and revealed by Coomassie blue staining. The GST-tagged protein and nucleotide used are indicated at the top of each lane. The migration of the individual proteins is indicated on the right of the panels. (G) ^{35}S-labeled 15.5K, fibrillarin, NOP56, and NOP58 were incubated with immobilized GST, GST-BCD1(1-360), GST-NUFIP, GST-TAF9, or GST-NOP17. Bound proteins were eluted, resolved by SDS-PAGE, and revealed by autoradiography. The GST-protein used is indicated above each lane. The identity of the radiolabeled protein is indicated on the left of the panel. The asterisk denotes nonspecific material that is sometimes seen with the NOP56 and NOP58 in vitro-translated proteins. Input, 10% of the input material. Note that a single exposure of one gel was used for each individual translated protein.

and N terminus present in GST-BCD1(1-360) are insufficient for this interaction. Taken together, our data indicate that a number of contacts are made between the novel pre-snoRNP factors and the core box C/D proteins. In particular, NUFIP appears to interact with all four core box C/D proteins and could, therefore, play a significant role as a bridging factor in snoRNP assembly.

NUFIP mediates the assembly of partially reconstituted pre-snoRNP complexes. Analysis of the protein-protein interactions in the pre-snoRNP revealed that several proteins potentially interact with multiple factors in the pre-snoRNP. In particular, NUFIP is capable of interacting with many factors, including all of the core box C/D proteins, and could function as a bridging factor or scaffold protein in box C/D snoRNP assembly. We therefore investigated whether NUFIP could bridge the interaction between 15.5K and either NOP56 or NOP58 in a reconstituted pre-snoRNP in the presence of a box C/D snoRNA. For these experiments we used deletion mutants of NOP56 [NOP56(1-458)] and NOP58 [NOP58(1-435)], which lack the C-terminal charged region. This region of each protein is not essential for snoRNP formation in yeast (15, 32), and the truncated human proteins are significantly more soluble than the full-length polypeptides (data not shown). Polyhistidine-thioredoxin-tagged NOP56(1-458) or NOP58(1-435) (Fig. 6A), GST-NUFIP, and 15.5K were sequentially added to MagZ beads (magnetic beads that bind polyhistidine-tagged proteins). The complexes assembled on the beads were then incubated with ^{32}P-labeled U14 or U14 MutC snoRNAs. The U14 MutC snoRNA contains a mutation in the conserved GA nucleotides of box C that abolishes 15.5K protein binding (50). Bound RNAs were isolated and analyzed by denaturing PAGE and revealed by autoradiography.

Significant levels of ^{32}P-labeled U14 snoRNA were bound when 15.5K, NUFIP, and either NOP56(1-458) or NOP58(1-435) were assembled onto MagZ beads (Fig. 6B and C, lanes 9). Only background levels of the U14 snoRNA were bound by the MagZ beads alone (lane 2). The absence of one or more of the proteins severely reduced or abolished the association with the U14 snoRNA. A weak signal was consistently observed when 15.5K and NUFIP were used in the absence of NOP56 or NOP58. NUFIP possesses a zinc-finger motif, and the recombinant protein has a weak affinity of the MagZ beads,

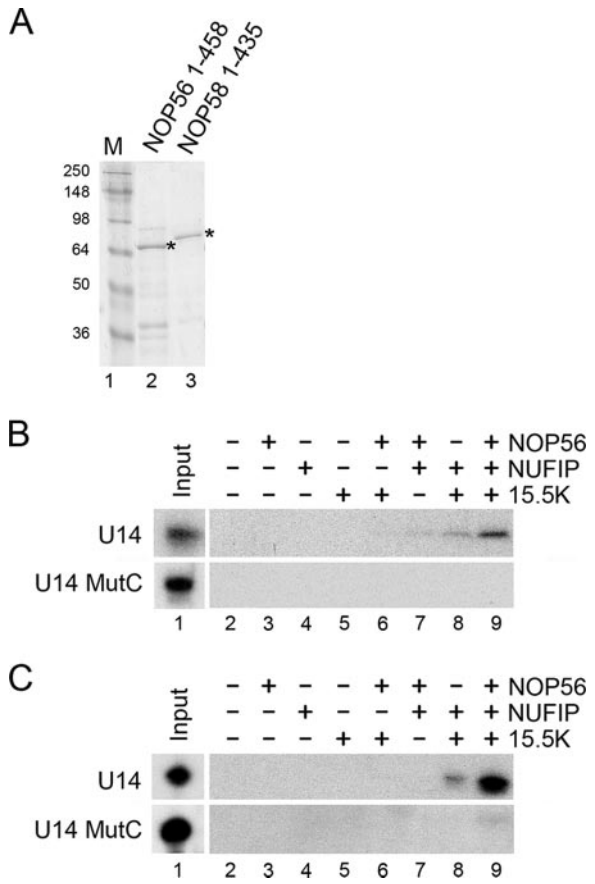

FIG. 6. NUFIP bridges interactions between both NOP56 and NOP58 and 15.5K. (A) Recombinant thioredoxin-tagged NOP56(1-458) and NOP58(1-435) were separated by SDS-PAGE and visualized by Coomassie blue staining. Full-length proteins are indicated by an asterisk. The protein loaded is indicated at the top of the gel. M, molecular weight marker. The sizes are indicated to the left in kilodaltons. (B and C) In vitro assembly of a partial pre-snoRNP complex. Thioredoxin-tagged (A) NOP56(1-458) or (B) NOP58(1-435) were immobilized onto MagZ beads with GST-NUFIP and 15.5K added successively. The beads were then incubated with ^{32}P-labeled U14 wild-type or U14 mutC transcripts. Bound RNA was recovered, separated on an 8% polyacrylamide–7 M urea gel, and visualized by autoradiography. The RNA used is indicated on the left of each panel. The proteins added to each reaction are indicated above each lane. Input, 10% of the input material.

leading to a low-level retention of the U14 snoRNA in the presence of 15.5K. However, this signal was always considerably lower that that seen when all three proteins were present. None of the combinations of proteins bound the U14 MutC snoRNA (Fig. 6B and C, lanes 3 to 8), confirming that the formation of either the NOP56-NUFIP-15.5K-U14 or the NOP58-NUFIP-15.5K-U14 snoRNA complex is dependent on a functional box C/D motif. These results show that NUFIP can simultaneously and directly interact with core box C/D proteins to mediate the formation of partial pre-snoRNP complexes.

DISCUSSION

Characterization of four novel box C/D snoRNP biogenesis factors. Here, we report four novel biogenesis factors—BCD1, NOP17, NUFIP. and TAF9—associated with U3 and U8 pre-snoRNP complexes present in nuclear extracts. These proteins were not associated with mature nucleolar U3 and U8 snoRNPs, indicating that they dissociate before nucleolar localization and are, therefore, involved in snoRNP biogenesis rather than function. Using RNAi, we show that BCD1 and NOP17 are essential for the accumulation of independently transcribed (U3 and U8) and intronic (U14) snoRNAs, indicating that they are general box C/D snoRNP biogenesis factors. The RNAi analysis of NUFIP will be reported elsewhere (Boulon and Bertrand, unpublished). The RNAi-mediated depletion of NOP58, NOP17, and BCD1 resulted in a reduction in U3 snoRNA levels in Cajal bodies. This could be the result of either a loss of Cajal body localization or, more likely, a reduction in snoRNA levels in the nucleoplasm. These proteins are, therefore, critical for either the formation or the stability of the pre-snoRNP complex. In contrast, the U3 snoRNA is still present in Cajal bodies in fibrillarin-depleted cells. In addition, these cells contain higher levels of nucleoplasmic U3 snoRNA, suggesting that the loss of fibrillarin results in a defect in biogenesis and/or localization. This may lead to reduced levels of production of the mature complex but not destabilization of the pre-snoRNA. NUFIP has been demonstrated to be present in the nucleoplasm of mouse cells. Unfortunately, the antibodies used in this present study did not function in immunofluorescence studies, and we could not determine their subcellular localization.

BCD1, NOP17, NUFIP, and TAF9 all interact with the core box C/D proteins as well as either TIP48 and/or TIP49, suggesting that they may play a role in bridging interactions within the pre-snoRNP. All four factors are associated with the U3 pre-snoRNA and the longest form of the U8 pre-snoRNA, which probably is the primary transcript (49a). This observation is consistent with a role for these proteins in the early stages of pre-snoRNP assembly, possibly in the initial recruitment of the box C/D core proteins NOP56, NOP58, and/or fibrillarin. Consistent with this, BCD1, NOP17, NUFIP, TAF9, TIP48, and TIP49 are all present in affinity-purified NOP58 complexes. NOP17, NUFIP, TAF9, TIP48, and TIP49 have been proposed to be involved in either RNA polymerase II transcription and/or chromatin remodeling (6, 14, 26, 27, 54, 55). Although it is possible that each of these proteins has independent roles in transcription and/or chromatin remodeling and snoRNP biogenesis, it is interesting to speculate that these factors may provide a link between snoRNA transcription and snoRNP assembly. NOP17 was previously shown to be involved in rRNA processing and not to be important for snoRNA accumulation in *S. cerevisiae* (16). Although we cannot comment on the role of human NOP17 in ribosome biogenesis, our data indicate that NOP17 is required for box C/D snoRNA accumulation in HeLa cells and is, therefore, involved in snoRNP biogenesis.

A dynamic pre-snoRNP interaction network. We have used a combination of purified GST-tagged proteins and in vitro-translated proteins to analyze the protein-protein interactions in the box C/D pre-snoRNP. This revealed an intricate network of 21 potential protein-protein interactions within the mammalian pre-snoRNP complex (summarized in Fig. 7). The factors analyzed include the core box C/D proteins and six snoRNP assembly proteins (TIP48, TIP49, NOP17, BCD1,

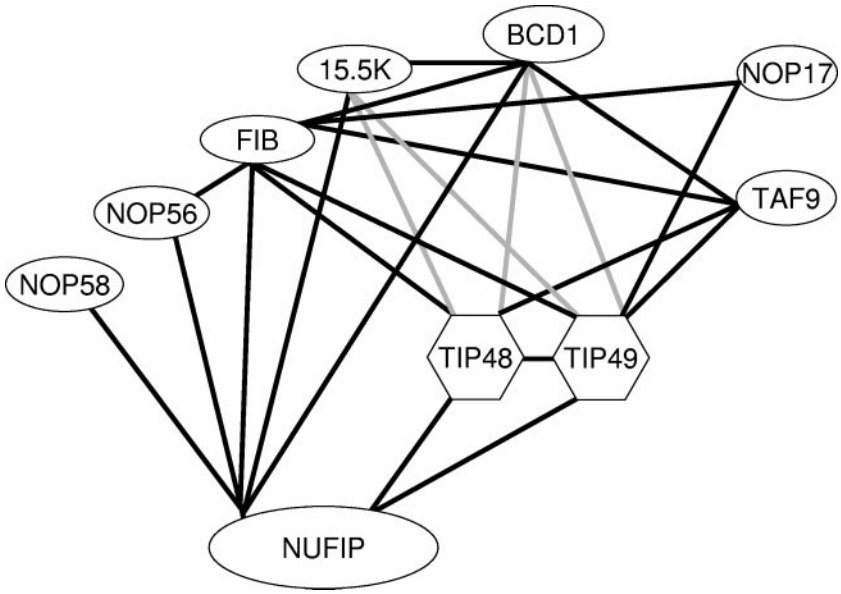

FIG. 7. Schematic representation of the box C/D pre-snoRNP interaction network. The protein-protein interaction data produced during the present study are represented schematically. Black lines represent interactions between individual proteins. Gray lines indicate protein-protein interactions that are altered by the nucleotide bound to either TIP48 or TIP49.

NUFIP, and TAF9). In most cases the interactions described are reciprocal; for example, GST-tagged NUFIP binds in vitro-translated 15.5K (Fig. 5G), and GST-15.5K binds in vitro-translated NUFIP (data not shown). Several of the interactions were also observed between proteins overexpressed and purified from *E. coli* (Fig. 2, 5, and 6 and data not shown), suggesting that the interactions observed using the proteins expressed in reticulocyte lysate are direct. However, these experiments were limited by the fact that we could not generate soluble full-length GST-fusion proteins of BCD1, NOP56, and NOP58. The use of in vitro-translated proteins in combination with the GST fusion proteins revealed an extensive series of interactions between the new box C/D snoRNP biogenesis factors (BCD1, NOP17, NUFIP, and TAF9) and the core box C/D proteins (Fig. 7). Furthermore, the novel pre-snoRNP factors also interacted with TIP48 and/or TIP49. Interestingly, TIP48 and TIP49, whose recruitment to the pre-snoRNP was shown previously to be linked to NOP56 and NOP58, were both shown to interact with fibrillarin and 15.5K but not NOP56 and NOP58. The biogenesis factors BCD1, NUFIP, TIP48, and TIP49 appear central to the protein-protein interaction scheme. This is especially true for NUFIP, which interacts with all four of the core box C/D snoRNP proteins (Fig. 7). In addition, all four of these pre-snoRNP proteins are capable of multimerization. Most notable among these are TIP48 and TIP49, which are proposed to interact to form a double hexameric complex (24; K. S. McKeegan and N. J. Watkins, unpublished data). As such, we believe that these proteins may form an extensive and potentially repeating scaffold around which the pre-snoRNP is assembled (see below).

The only interaction we observed between the individual core box C/D proteins was between NOP56 and fibrillarin. The lack of detectable interactions between the other core box C/D proteins is surprising given the suggested role for protein-protein interactions in snoRNP assembly. Furthermore, NOP58 and fibrillarin have been shown to cross-link to adjacent nucleotides on the opposite sides of stem II of the box C/D motif, suggesting a close proximity in the mature complex (7). Work with both yeast and mammalian cell extracts has shown that NOP56 and fibrillarin recruitment to the snoRNA are linked (32, 48).

The AAA+-like proteins TIP48 and TIP48 are expected to be involved in the ATP-dependent remodeling and rearrangement of large protein-protein complexes. A variety of nucleotides have been shown to induce conformational changes to AAA+ complexes that represent different stages of their ATP-hydrolysis cycle. Using different nucleotide analogues we analyzed the dynamics of the protein interactions of both GST-TIP48 and GST-TIP49 (Fig. 7, gray lines). 15.5K preferentially interacted with both TIP48 and TIP49 in the presence of ATP. In contrast, BCD1 interacted preferentially with TIP48 and TIP49 in the presence of ADP and ATP, respectively. This indicates ATP binding and hydrolysis intricately regulates the dynamic protein-protein interactions within the pre-snoRNP. These results support the previous observation that ATP hydrolysis by both TIP48 and TIP49 is important for snoRNP biogenesis in yeast (28). Since many AAA+ proteins function through adaptor proteins (12), it is likely that TIP48 and TIP49 interact directly with 15.5K and fibrillarin but require other pre-snoRNP proteins such as NUFIP if they act upon NOP56 and NOP58. Since both U3 and U8 box C/D snoRNP biogenesis involves the dynamic recruitment and release of multiple factors, it is likely that TIP48 and/or TIP49, as the only ATPases identified in the pre-snoRNP, coordinate this process through the binding, hydrolysis, and release of nucleotides (49). TIP48 and TIP49 have also been implicated to function linking pre-mRNA splicing to snoRNP assembly. NOP17 and BCD1 are essential for intronic U14 snoRNA accumulation. This suggests that the interaction network is applicable to the biogenesis of box C/D snoRNAs encoded in pre-mRNA in-

trons. However, the direct involvement of many of these factors in intronic snoRNP biogenesis has yet to be established.

Remodeling the core box C/D snoRNP complex. One possible explanation for the lack of detectable interactions between the core box C/D factors is that the isolated proteins are not in a conformation that is representative of that found in the mature snoRNP. These proteins may be structurally remodeled during snoRNP biogenesis to allow stable integration into the box C/D snoRNP complex. This hypothesis is supported by the large number of interactions between the core box C/D proteins and the assembly or biogenesis factors. Furthermore, we demonstrate that NUFIP can simultaneously interact with both 15.5K and either NOP56 or NOP58, enabling us to build a partial box C/D snoRNP. It is therefore likely that the biogenesis factors interact to form a scaffold around which the snoRNP is assembled. Due to its interaction with all four core proteins, we propose that NUFIP plays a central role in this scaffold. However, given the essential role for BCD1 and NOP17 in this process, it is likely that they also contribute significantly to the recruitment of the core box C/D proteins. We propose that during biogenesis a restructuring or remodeling event occurs in the pre-snoRNP that results in the stable docking of the core proteins into the box C/D snoRNP. This would probably coincide with the release of the remaining biogenesis factors and the localization of the completed complex to the nucleolus. Evidence for a remodeling and/or restructuring step to U3 box C/D snoRNP biogenesis has been presented (49). Furthermore, the finding that this change in the stability of protein association also occurs during U8 snoRNP biogenesis suggests that this event may occur in the formation of all members of this class of complex. We propose that this difference in stability of protein association reflects two stages of snoRNP assembly. The less stable complex probably corresponds to the core proteins being held in the pre-snoRNP complex through their interactions with biogenesis factors such as NUFIP. During the latter stages of biogenesis, remodeling of NOP56 and NOP58 creates a stable snoRNP. It was previously suggested that TIP49, as the only ATPase associated with the latter stages of U3 snoRNP biogenesis, drives this structural change (49). Our current data support this idea and indicate that TIP49 is capable of mediating dynamic interactions within the pre-snoRNP complex via interactions with both the core proteins (15.5K and fibrillarin) and biogenesis factors (Fig. 7).

Although our data provide strong evidence for restructuring of the core box C/D snoRNP complex during biogenesis, the molecular nature of this change is unclear. Interestingly, the *Archaea* box C/D complexes assemble in the absence of assembly factors. This, therefore, suggests that the structure of one or more of the core box C/D proteins is altered during snoRNP biogenesis. AAA+ proteins, such as those present in clamp-loading complexes or involved in protein degradation, are molecular machines that function in the structural rearrangement of proteins and protein-nucleic acid complexes during their assembly or disassembly (12, 19, 43). As such, TIP48 and/or TIP49 are capable, in theory, of structurally altering the core complex. This restructuring probably creates a high-affinity binding site in one or more of the core proteins that stabilize the snoRNP complex. Interestingly, a restructuring or remodeling event has been proposed to occur during ATP-dependent assembly of Sm proteins onto the spliceosomal snRNPs (36, 53), suggesting that this may be a common feature of RNP assembly.

ACKNOWLEDGMENTS

We thank Susan Baserga, Pavel Cabart, Sander Granneman, Ed Hurt, Reinhard Lührmann, Stuart Maxwell, Ger Pruijn, and Robert Tjian for generously providing plasmids. We thank Reinhard Lührmann and Ira Lemm for generously providing cell extracts, hPRP31 siRNAs, and the fluorescently labeled U4 snRNA probe and Barbara Bardoni for providing NUFIP antibodies. We also thank Jeremy Brown, Hannah Richardson, and Claudia Schneider for critically reading the manuscript.

This study was supported by grants from the BBSRC and Royal Society.

REFERENCES

1. **Aittaleb, M., R. Rashid, Q. Chen, J. R. Palmer, C. J. Daniels, and H. Li.** 2003. Structure and function of archaeal box C/D sRNP core proteins. Nat. Struct. Biol. **10:**256–263.
2. **Bachellerie, J. P., J. Cavaille, and A. Huttenhofer.** 2002. The expanding snoRNA world. Biochimie **84:**775–790.
3. **Bardoni, B., A. Schenck, and J. L. Mandel.** 1999. A novel RNA-binding nuclear protein that interacts with the fragile X mental retardation (FMR1) protein. Hum. Mol. Genet. **8:**2557–2566.
4. **Boulon, S., C. Verheggen, B. E. Jady, C. Girard, C. Pescia, C. Paul, J. K. Ospina, T. Kiss, A. G. Matera, R. Bordonne, and E. Bertrand.** 2004. PHAX and CRM1 are required sequentially to transport U3 snoRNA to nucleoli. Mol. Cell **16:**777–787.
5. **Brown, J. D.** 2001. Ribosome biogenesis: stripping for AAAction? Curr. Biol. **11:**R710–R712.
6. **Cabart, P., H. K. Chew, and S. Murphy.** 2004. BRCA1 cooperates with NUFIP and P-TEFb to activate transcription by RNA polymerase II. Oncogene **23:**5316–5329.
7. **Cahill, N. M., K. Friend, W. Speckmann, Z. H. Li, R. M. Terns, M. P. Terns, and J. A. Steitz.** 2002. Site-specific cross-linking analyses reveal an asymmetric protein distribution for a box C/D snoRNP. EMBO J. **21:**3816–3828.
8. **Cordin, O., J. Banroques, N. K. Tanner, and P. Linder.** 2006. The DEAD-box protein family of RNA helicases. Gene **367:**17–37.
9. **Dennis, P. P., and A. Omer.** 2005. Small non-coding RNAs in *Archaea*. Curr. Opin. Microbiol. **8:**685–694.
10. **Dignam, J. D., R. M. Lebovitz, and R. G. Roeder.** 1983. Accurate transcription initiation by RNA polymerase II in a soluble extract from isolated mammalian nuclei. Nucleic Acids Res. **11:**1475–1489.
11. **Elbashir, S. M., J. Harborth, K. Weber, and T. Tuschl.** 2002. Analysis of gene function in somatic mammalian cells using small interfering RNAs. Methods **26:**199–213.
12. **Erzberger, J. P., M. L. Mott, and J. M. Berger.** 2006. Structural basis for ATP-dependent DnaA assembly and replication-origin remodeling. Nat. Struct. Mol. Biol. **13:**676–683.
13. **Filipowicz, W., and V. Pogacic.** 2002. Biogenesis of small nucleolar ribonucleoproteins. Curr. Opin. Cell Biol. **14:**319–327.
14. **Frank, S. R., T. Parisi, S. Taubert, P. Fernandez, M. Fuchs, H. M. Chan, D. M. Livingston, and B. Amati.** 2003. MYC recruits the TIP60 histone acetyltransferase complex to chromatin. EMBO Rep. **4:**575–580.
15. **Gautier, T., T. Berges, D. Tollervey, and E. Hurt.** 1997. Nucleolar KKE/D repeat proteins Nop56p and Nop58p interact with Nop1p and are required for ribosome biogenesis. Mol. Cell. Biol. **17:**7088–7098.
16. **Gonzales, F. A., N. I. Zanchin, J. S. Luz, and C. C. Oliveira.** 2005. Characterization of *Saccharomyces cerevisiae* Nop17p, a novel Nop58p-interacting protein that is involved in pre-rRNA processing. J. Mol. Biol. **346:**437–455.
17. **Granneman, S., and S. J. Baserga.** 2004. Ribosome biogenesis: of knobs and RNA processing. Exp. Cell Res. **296:**43–50.
18. **Granneman, S., J. Vogelzangs, R. Lührmann, W. J. van Venrooij, G. J. Pruijn, and N. J. Watkins.** 2004. Role of pre-rRNA base pairing and 80S complex formation in subnucleolar localization of the U3 snoRNP. Mol. Cell. Biol. **24:**8600–8610.
19. **Hanson, P. I., and S. W. Whiteheart.** 2005. AAA+ proteins: have engine, will work. Nat. Rev. Mol. Cell. Biol. **6:**519–529.
20. **Hiley, S. L., T. Babak, and T. R. Hughes.** 2005. Global analysis of yeast RNA processing identifies new targets of RNase III and uncovers a link between tRNA 5′ end processing and tRNA splicing. Nucleic Acids Res. **33:**3048–3056.
21. **Hirose, T., T. Ideue, M. Nagai, M. Hagiwara, M. D. Shu, and J. A. Steitz.** 2006. A spliceosomal intron binding protein, IBP160, links position-dependent assembly of intron-encoded box C/D snoRNP to pre-mRNA splicing. Mol. Cell **23:**673–684.
22. **Hirose, T., M. D. Shu, and J. A. Steitz.** 2003. Splicing-dependent and -inde-

pendent modes of assembly for intron-encoded box C/D snoRNPs in mammalian cells. Mol. Cell **12:**113–123.
23. **Hirose, T., and J. A. Steitz.** 2001. Position within the host intron is critical for efficient processing of box C/D snoRNAs in mammalian cells. Proc. Natl. Acad. Sci. USA **98:**12914–12919.
24. **Ikura, T., V. V. Ogryzko, M. Grigoriev, R. Groisman, J. Wang, M. Horikoshi, R. Scully, J. Qin, and Y. Nakatani.** 2000. Involvement of the TIP60 histone acetylase complex in DNA repair and apoptosis. Cell **102:**463–473.
25. **Ito, T., T. Chiba, R. Ozawa, M. Yoshida, M. Hattori, and Y. Sakaki.** 2001. A comprehensive two-hybrid analysis to explore the yeast protein interactome. Proc. Natl. Acad. Sci. USA **98:**4569–4574.
26. **Jonsson, Z. O., S. K. Dhar, G. J. Narlikar, R. Auty, N. Wagle, D. Pellman, R. E. Pratt, R. Kingston, and A. Dutta.** 2001. Rvb1p and Rvb2p are essential components of a chromatin remodeling complex that regulates transcription of over 5% of yeast genes. J. Biol. Chem. **276:**16279–16288.
27. **Jonsson, Z. O., S. Jha, J. A. Wohlschlegel, and A. Dutta.** 2004. Rvb1p/Rvb2p recruit Arp5p and assemble a functional Ino80 chromatin remodeling complex. Mol. Cell **16:**465–477.
28. **King, T. H., W. A. Decatur, E. Bertrand, E. S. Maxwell, and M. J. Fournier.** 2001. A well-connected and conserved nucleoplasmic helicase is required for production of box C/D and H/ACA snoRNAs and localization of snoRNP proteins. Mol. Cell. Biol. **21:**7731–7746.
29. **Kiss, T.** 2004. Biogenesis of small nuclear RNPs. J. Cell Sci. **117:**5949–5951.
30. **Kiss, T.** 2002. Small nucleolar RNAs: an abundant group of noncoding RNAs with diverse cellular functions. Cell **109:**145–148.
31. **Klemm, R. D., J. A. Goodrich, S. Zhou, and R. Tjian.** 1995. Molecular cloning and expression of the 32-kDa subunit of human TFIID reveals interactions with VP16 and TFIIB that mediate transcriptional activation. Proc. Natl. Acad. Sci. USA **92:**5788–5792.
32. **Lafontaine, D. L., and D. Tollervey.** 2000. Synthesis and assembly of the box C+D small nucleolar RNPs. Mol. Cell. Biol. **20:**2650–2659.
33. **Liu, S., R. Rauhut, H. P. Vornlocher, and R. Luhrmann.** 2006. The network of protein-protein interactions within the human U4/U6.U5 tri-snRNP. RNA **12:**1418–1430.
34. **Lyman, S. K., L. Gerace, and S. J. Baserga.** 1999. Human Nop5/Nop58 is a component common to the box C/D small nucleolar ribonucleoproteins. RNA **5:**1597–1604.
35. **Maxwell, E. S., and M. J. Fournier.** 1995. The small nucleolar RNAs. Annu. Rev. Biochem. **64:**897–934.
36. **Meister, G., C. Eggert, and U. Fischer.** 2002. SMN-mediated assembly of RNPs: a complex story. Trends Cell Biol. **12:**472–478.
37. **Nazar, R. N.** 2004. Ribosomal RNA processing and ribosome biogenesis in eukaryotes. IUBMB Life **56:**457–465.
38. **Newman, D. R., J. F. Kuhn, G. M. Shanab, and E. S. Maxwell.** 2000. Box C/D snoRNA-associated proteins: two pairs of evolutionarily ancient proteins and possible links to replication and transcription. RNA **6:**861–879.
39. **Nottrott, S., K. Hartmuth, P. Fabrizio, H. Urlaub, I. Vidovic, R. Ficner, and R. Luhrmann.** 1999. Functional interaction of a novel 15.5kD [U4/U6.U5] tri-snRNP protein with the 5′ stem-loop of U4 snRNA. EMBO J. **18:**6119–6133.
40. **Omer, A. D., S. Ziesche, H. Ebhardt, and P. P. Dennis.** 2002. In vitro reconstitution and activity of a C/D box methylation guide ribonucleoprotein complex. Proc. Natl. Acad. Sci. USA **99:**5289–5294.
41. **Peng, W. T., M. D. Robinson, S. Mnaimneh, N. J. Krogan, G. Cagney, Q. Morris, A. P. Davierwala, J. Grigull, X. Yang, W. Zhang, N. Mitsakakis, O. W. Ryan, N. Datta, V. Jojic, C. Pal, V. Canadien, D. Richards, B. Beattie, L. F. Wu, S. J. Altschuler, S. Roweis, B. J. Frey, A. Emili, J. F. Greenblatt, and T. R. Hughes.** 2003. A panoramic view of yeast noncoding RNA processing. Cell **113:**919–933.
42. **Rashid, R., M. Aittaleb, Q. Chen, K. Spiegel, B. Demeler, and H. Li.** 2003. Functional requirement for symmetric assembly of archaeal box C/D small ribonucleoprotein particles. J. Mol. Biol. **333:**295–306.
43. **Sauer, R. T., D. N. Bolon, B. M. Burton, R. E. Burton, J. M. Flynn, R. A. Grant, G. L. Hersch, S. A. Joshi, J. A. Kenniston, I. Levchenko, S. B. Neher, E. S. Oakes, S. M. Siddiqui, D. A. Wah, and T. A. Baker.** 2004. Sculpting the proteome with AAA(+) proteases and disassembly machines. Cell **119:**9–18.
44. **Schaffert, N., M. Hossbach, R. Heintzmann, T. Achsel, and R. Lührmann.** 2004. RNAi knockdown of hPrp31 leads to an accumulation of U4/U6 di-snRNPs in Cajal bodies. EMBO J. **23:**3000–3009.
45. **Schultz, A., S. Nottrott, N. J. Watkins, and R. Lührmann.** 2006. Protein-protein and protein-RNA contacts both contribute to the 15.5K-mediated assembly of the U4/U6 snRNP and the box C/D snoRNPs. Mol. Cell. Biol. **26:**5146–5154.
46. **Terns, M. P., and R. M. Terns.** 2002. Small nucleolar RNAs: versatile *trans*-acting molecules of ancient evolutionary origin. Gene Expr. **10:**17–39.
47. **Tran, E. J., X. Zhang, and E. S. Maxwell.** 2003. Efficient RNA 2′-O-methylation requires juxtaposed and symmetrically assembled archaeal box C/D and C′/D′ RNPs. EMBO J. **22:**3930–3940.
48. **Watkins, N. J., A. Dickmanns, and R. Lührmann.** 2002. Conserved stem II of the box C/D motif is essential for nucleolar localization and is required, along with the 15.5K protein, for the hierarchical assembly of the box C/D snoRNP. Mol. Cell. Biol. **22:**8342–8352.
49. **Watkins, N. J., I. Lemm, D. Ingelfinger, C. Schneider, M. Hossbach, H. Urlaub, and R. Lührmann.** 2004. Assembly and maturation of the U3 snoRNP in the nucleoplasm in a large dynamic multiprotein complex. Mol. Cell **16:**789–798.
49a. **Watkins, N. J., I. Lemm, and R. Lührmann.** Involvement of nuclear import and export factors in U8 box C/D snoRNP biogenesis. Mol. Cell. Biol., in press.
50. **Watkins, N. J., V. Segault, B. Charpentier, S. Nottrott, P. Fabrizio, A. Bachi, M. Wilm, M. Rosbash, C. Branlant, and R. Lührmann.** 2000. A common core RNP structure shared between the small nucleolar box C/D RNPs and the spliceosomal U4 snRNP. Cell **103:**457–466.
51. **Weinstein, L. B., and J. A. Steitz.** 1999. Guided tours: from precursor snoRNA to functional snoRNP. Curr. Opin. Cell Biol. **11:**378–384.
52. **Will, C. L., and R. Luhrmann.** 2001. Molecular biology. RNP remodeling with DExH/D boxes. Science **291:**1916–1917.
53. **Yong, J., L. Wan, and G. Dreyfuss.** 2004. Why do cells need an assembly machine for RNA-protein complexes? Trends Cell Biol. **14:**226–232.
54. **Zhao, R., M. Davey, Y. C. Hsu, P. Kaplanek, A. Tong, A. B. Parsons, N. Krogan, G. Cagney, D. Mai, J. Greenblatt, C. Boone, A. Emili, and W. A. Houry.** 2005. Navigating the chaperone network: an integrative map of physical and genetic interactions mediated by the hsp90 chaperone. Cell **120:**715–727.
55. **Zhao, R., and W. A. Houry.** 2005. Hsp90: a chaperone for protein folding and gene regulation. Biochem. Cell Biol. **83:**703–710.